Available online at www.sciencedirect.com
ScienceDirect
Journal of the European Ceramic Society 31 (2011) 1849–1855
www.elsevier.com/locate/jeurceramsoc

Short Communication

The role of zircon particle size distribution, surface area and contamination on the properties of silica–zircon ceramic materials

P.J. Wilson [a,b,*], S. Blackburn [a], R.W. Greenwood [a], B. Prajapti [b], K. Smalley [b]

[a] *University of Birmingham, Department of Chemical Engineering, Edgbaston, Birmingham B15 2TT, United Kingdom*
[b] *Ross Ceramic Ltd., Derby Road, Denby DE5 8NX, United Kingdom*

Received 3 September 2010; received in revised form 23 February 2011; accepted 2 March 2011
Available online 3 April 2011

Abstract

Zircon is used as an additive to silica ceramics for use in investment casting to improve their high temperature properties. However, little is known about the mechanisms by which this occurs. To investigate the effect of zircon addition to a silica ceramic a number of silica–zircon formulations were created utilising three different batches of zircon with different particle size distributions (PSDs), surface areas and contaminant inclusions. The contaminant inclusion of the zircon, present in the zircon from the ball-milling stage of manufacture, appeared to have a large effect on the room temperature flexural strength, high temperature flexural strength and high temperature creep properties. It is also suggested that any increase in post-fired cristobalite content and any change to crystal growth morphology was due to the inherent contaminant inclusions and not because of the zircon itself. Hence, use of silica–zircon materials in ceramics for investment casting should account for variation in the contaminant inclusion of the zircon in order to maintain the specific material properties required.

Keywords: D. Al_2O_3; D. SiO_2; C. Mechanical properties; B. Impurities; D. Silicate

1. Introduction

Zircon, or zirconium silicate [$ZrSiO_4$], is an extremely common additive used in the investment casting industry. It is used in ceramic core formulations as well as a face coat and stucco material for the shell materials that are also used for investment casting.[1] Zircon is useful for investment casting due to its low coefficient of thermal expansion ($\approx 4.1 \times 10^{-6}\,^{\circ}C^{-1}$ between 25 °C and 1400 °C), its low coefficient of heat conductivity (5.1 W m^{-1} °C^{-1} at 25 °C and 3.5 W m^{-1} °C^{-1} at 1000 °C) and its lack of phase transformations up to 1687 ± 7 °C.[2]

Zircon is a common mineral in the majority of igneous and metamorphic rocks, but is also a host for a significant proportion of whole-rock abundances of uranium, thorium, hafnium and other rare earth elements.[3] For this reason zircon is generally not available more than 98% pure, the bulk of the 2% impurity is made up of Hafnium Silicate, which is chemically identical to zircon up to ≈1627 °C.[4] Zircon is also known to hold adsorbed water and chemically bonded hydroxyl groups; these can release water at either a steady rate with increasing temperature or exhibit a two phase loss, with adsorbed water removal at low temperatures and OH^- groups at higher temperatures, depending on the source.[5]

Impurities of U and Th are well known to have common radioactive isotopes, which are abundant in natural zircon. α-Radiation from these isotopes can induce a phase change in the zircon crystal structure, turning it into a third class of naturally occurring amorphous material, known as metamict.[6] These decay events cause atoms within the crystal lattice structure to become dislocated, typically between 700 and 2000 per α-particle.[7] Radiation damage in zircon not only disrupts the crystal structure and causes the overall system to become aperiodic, but also causes changes to the overall bulk properties of the zircon.[8]

During grinding operations, such as the manufacturing technique of ball milling, contamination from wear of the milling media and lining of the mill itself can generate contamination which is subsequently included into the mill products.[9,10] The exact amount of contamination depends on the length of time

* Corresponding author at: University of Birmingham, Department of Chemical Engineering, Edgbaston, Birmingham B15 2TT, United Kingdom. Tel.: +44 01214711922.
E-mail address: pjw256@gmail.com (P.J. Wilson).

0955-2219/$ – see front matter © 2011 Elsevier Ltd. All rights reserved.
doi:10.1016/j.jeurceramsoc.2011.03.005

Table 1
Properties of the 3 zircon batches used.

Zircon	1	2	3
Crystallinity (%)	100	100	100
TiO_2 (%)	0.11	0.12	0.18
Al_2O_3 (%)	0.75	0.11	0.12
Fe_2O_3 (%)	0.06	0.05	0.09
Na_2O (%)	0.24	ND	ND
Y_2O_3 (%)	0.12	ND	0.13
Total contamination (%)	1.28	0.28	0.52
Surface area (m^2/g)	0.62	1.00	4.17
D_{50} (μm)	20.1	19.8	4.1
Circularity	0.64	0.64	0.62

a material is milled, the size of the mill media, the mill media material, the mill lining material and the current wear of the media itself. This last point is due to full scale industrial mills adding media to maintain an equilibrium mass of media inside the mill, resulting in uneven, and non-reproducible, wear of the mill media present at any given time.[11] Wear during dry grinding has been shown to be entirely due to abrasion and erosion of the mill media and mill lining.[12]

The contamination from this operation can be of significance, especially in materials that rely on their purity for successful operation. The contamination from ball milling has been shown to affect high temperature properties in some ceramic materials,[13] but not for silica based ceramics used in the investment casting environment.

This study investigates the function of zircon weight percentage and surface area on the properties of silica ceramic materials created via the injection molding method. The effect of naturally occuring contaminants on the ceramic properties and crystallisation behaviour is also investigated. It has been shown that contaminants from within the zircon raw material batches can have a significant effect on investment casting shell mould integrity.[1]

2. Experimental procedure

2.1. Ceramic materials

The ceramic materials investigated were composed primarily of amorphous silica with an addition of zircon. The silica was obtained from Unimin Corporation, Camden, Tennessee, in a variety of particle size distributions that were obtained by ball milling with alumina grinding media and in an alumina lined mill, the purity of the silica is quoted as >99.7%, with <0.1% crystalline content. The different silica particle size distributions were mixed in such a way as to obtain a near identical PSD for every material created, including any zircon that was added to the system.

Additions of 5–25 wt% of three batches of zircon were added to a predominantly silica powder system. The 3 different zircon powders used are described in Table 1. The main differences in the zircon powders was in the way that they were prepared; zircon batch 1 was dry ball milled using alumina grinding media, zircon batch 2 was dry ball milled with silica grinding media and zircon batch 3 was wet ball milled with alumina grinding media, resulting in a finer particle size to batches 1 and 2. A comparison material made using only silica and no zircon addition was also created. (*N.B. 5 wt% zircon batch 3 was not created*).

The D_{50} of the zircon powders was determined by laser diffraction, see Section 2.9, the circularity was determined by SEM using polished, sintered ceramic specimens, see Section 2.8 and the crystallinity was determined by XRD, see Section 2.3.

The level of contamination in the zircon powders, as determined by XRF, was very different. The amount of TiO_2 and Fe_2O_3 was similar for all zircon batches, with a slightly larger amount present in zircon batch 3. Only zircon batch 1 had a detectable amount of Na_2O present, and batches 1 and 3 had a similar contamination level of Y_2O_3. However, the most significant contamination was the Al_2O_3, for zircon batch 1 the majority of the Al_2O_3 was from the dry ball milling of the zircon with alumina media, hence, the significantly higher amount present. Zircon batch 2 was ball milled in a silica lined ball mill with silica media, hence, the lower Al_2O_3 contamination level. However, a portion of undetectable free silica would be expected since this media would also be abraded in a similar manner to the alumina media used to ball mill batch 1. Zircon batch 3 was wet milled with alumina media and had significantly less detectable alumina contamination. However, any alumina present from the milling would most likely have a significantly smaller particle size than that from the dry milled zircon.

The materials were supplied from Ross Ceramics ltd. as fired test bars with dimensions, 100 mm × 12 mm × 4 mm. The test bars were all fired together up to approximately 1200 °C ± 25 °C and two separate fires were performed on each material formulation, in order that variation from the firing of the materials was included in the data.

2.2. X-ray fluorescence (XRF)

The XRF characterisation was conducted by Ceram (Stoke-on-Trent, UK), and was performed by forming the sample into a fused cast bead using Spectroflux 100B (1 part $Li_2B_4O_7$ to 4 parts $LiBO_2$ by weight) at a ratio of 5:1 to the sample, this allowed volatile components like Na_2O, K_2O, SO_3 and F to be retained. The sample preparation and analysis was conducted in accordance with the BS ISO 12677 standard for XRF analysis. This analysis was used to determine the level of contamination in the raw materials that were used.

2.3. XRD

Quantitative X-ray Diffraction was performed by Ceram (Stoke-on-Trent, UK). Prior to sending each sample for analysis, material from each kiln position was ground in a zirconia pestle and mortar and 1 g of each was mixed together. This gives the advantage of giving a batch average for a whole fire. At Ceram the material is then placed in a tungsten carbide TEMA mill and milled for 2 min, this is to reduce the particle size to 0.3–10 μm, to reduce micro-adsorption effects,[14] and to homogenise the sample. Alumina was used as the reference material.

2.4. Thermogravimetric analysis (TGA)

TGA analysis was performed in a Mettler Toledo TG50 combined furnace and balance with a Mettler Toledo TC15 controller box. Samples were dried in an oven at 110 °C for at least 24 h and then placed in a desiccator to cool. Open-topped alumina crucibles were filled to the top with the respective sample and placed inside the TGA. The heating rate used was 5 °C min^{-1} to the unit's maximum temperature of 1000 °C in accordance with Ek et al.[15] Six blank runs were also conducted using 2 different crucibles and this result subtracted from the sample measurements, of which an average of 3 measurements was taken.

2.5. Mechanical tests

Room temperature flexural strength tests were performed on the pre-formed test bars from Ross Ceramics using three-point fixtures, with rounded cylinders with a diameter of 6 mm and a cross head speed of 1 mm min^{-1}. Three point bend tests were also performed at 1475 °C using three point bend fixtures comprising re-crystallised alumina push rods and a custom furnace. This system was capable of isothermal hold temperatures up to 1500 °C. The span of the two support rods was 80 mm with a rounded knife edge and the test was performed at 1 mm min^{-1}.

Creep tests at 1475 °C were performed on the same rig as that used for the high temperature flexural tests. The load rate applied was 1 mm min^{-1} until a load of 3.2 N was achieved. This load was then held for 5 min and the total deflection of the test piece was recorded.

2.6. Pore size analysis

Mercury Porosimetry was used to determine the pore distribution of these materials both before and after heat treatment to 1570 °C for 20 min. The equipment used was a Micromeritics Autopore III. Samples were coarsely crushed in a pestle and mortar and dried in an oven at 120 °C for no less than 24 h. These were allowed to cool to room temperature before being placed in a penetrometer of known volume and intruded with mercury at 3450 Pa, in the low pressure portion of the test machine. The high pressure intrusion was then performed up to a pressure of approximately 207 MPa.

2.7. Dilatometry

Dilatometer measurements were conducted in a vertical dilatometer. Specimens were ground to approximately 20 mm × 4 mm × 4 mm.

Measurements were performed to 1600 °C to reveal the presence of any phase changes that may occur during casting and specifically to determine if the phase eutectic at 1587 °C of the SiO_2–Al_2O_3 systems was affecting material properties. Specimens were ramped to this temperature at 6 °C min^{-1} and held for 15 min before being cooled at 14 °C min^{-1}, this was as fast as the furnace would allow.

The total thermal contraction (TTC) during the test was taken by measuring the relative length change at 1250 °C during the heat-up of the material and again at 1250 °C during the cooling down of the sample after the dwell at 1600 °C.

2.8. SEM analysis (determining morphology of zircon powders)

Scanning election microscopy was performed on a JEOL 6060 SEM. Samples of fired and sintered ceramic were set in Epoxy resin, polished and coated with gold. A 20 kV electron beam was used with a spot size of 59 and backscattered electron images were obtained. ImgaeJ software was used to isolate the zircon particles in this material and determine the average circularity of the associated zircon powders the results of which are shown in Table 1.

2.9. Particle size analysis

Particle size analysis was performed on a Malvern Mastersizer 2000 laser diffraction particle size analyser; this technique determined the exact distribution of the powders used and their D_{50}. Samples for particle size analysis required no preparation since analysis was performed wet; this was standard procedure at Ross Ceramics. Samples were added to an agitated flask attached to the diffraction machine until the computer determined that the scatter signal was sufficient for measurement. 20 s of ultrasound with a wavelength of 20 μm were then applied to the sample before measurement.

2.10. Polarising optical microscopy

An Olympus BX51 petrological microscope was used to obtain optical micrographs using a plain polarising filter and a cross polarising filter with 1/4 wavelength advance were used to assess crystal growth in heat treated samples.

3. Results and discussion

3.1. Radiation damage of zircon

Samples of the raw zircon powders were heat treated to 1570 °C for 20 min, XRD was then performed to determine the amount of monoclinic zirconia present and compare to the XRD results obtained of the sample before heat treatment. Fig. 1 shows that the amount of zirconia present after heat treatment was significantly higher in zircon batch 3 than in zircon batches 1 or 2, which showed similar levels. This suggested that zircon batch 3 contained more metamict zircon than batches 1 or 2 and, hence, was more easily dissociated. This result was also supported by TGA analysis, which showed that zircon batch 3 released significantly more water upon heating to 1000 °C than either batches 1 or 2, see Fig. 2. The mass loss beyond 600 °C was from the release of internal OH^- ions, which indicated that more water was adsorbed into the zircons structure. The large amount of mass loss from 0 to 500 °C was most likely due to the significantly higher surface area of this zircon holding greater amounts of adsorbed water, most likely from the mill procedure, which was performed wet.

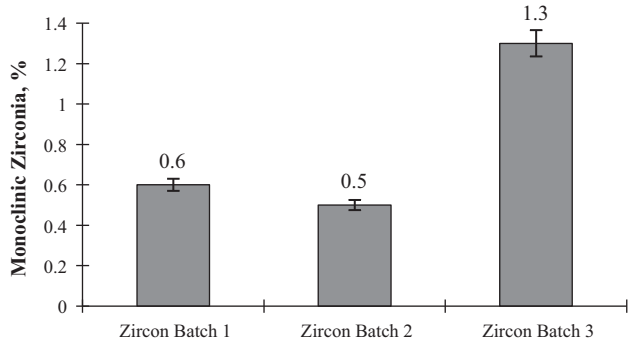

Fig. 1. Monoclinic zirconia level in zircon powders after heat treatment to 1570 °C for 30 min.

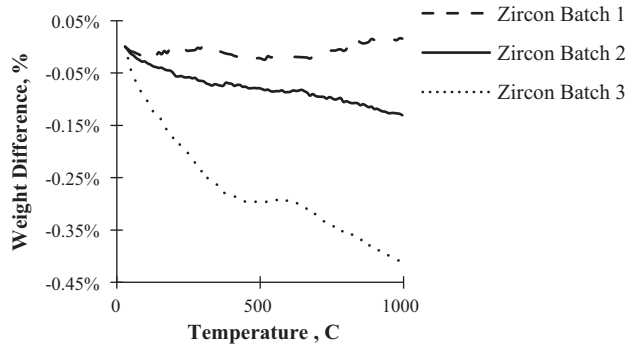

Fig. 2. TGA plot of zircon materials up to 1000 °C.

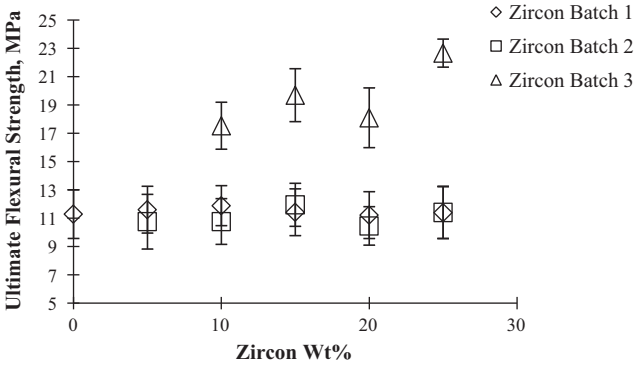

Fig. 3. Ultimate flexural strength of materials with the different zircon batches.

3.2. Zircon batch effect on flexural strength

The use of zircon batches 1 and 2 appeared to have little effect on the room temperature flexural strength of the ceramic materials regardless of addition, see Fig. 3. However, materials containing zircon batch 3 had considerably enhanced strength. This was most likely due to the finer size of the zircon batch 3 powder, which acted to increase the packing efficiency of the material; since this zircon was considerably finer than that of either batches 1 or 2, which had almost identical particle size distributions to each other.

The effect of the different contaminant inclusions from the zircon and the associated zircon surface area had a large effect on the flexural properties of these materials at 1475 °C. The strength at 1475 °C of materials containing zircon batches 1 and 2 can be seen to increase considerably with increasing amounts zircon, see Fig. 4. Materials containing zircon batch 2 were consistently stronger than those containing batch 1. This suggested that the strengthening mechanism was enhanced for materials containing zircon batch 2.

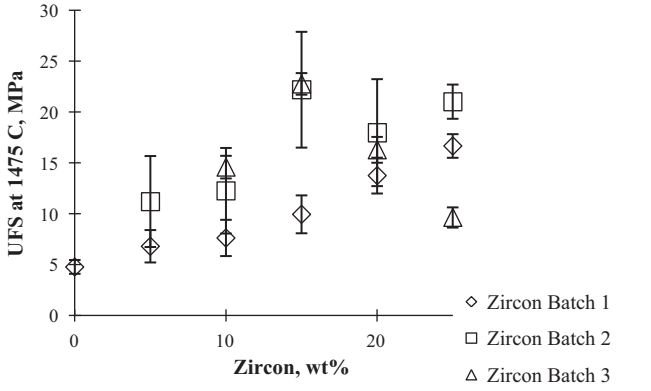

Fig. 4. The ultimate flexural strength of materials containing different amounts of zircon at 1475 °C.

The strength increase was caused by the increasing amount of contamination from the milling procedure of the two zircon batches. The alumina present within batch 1 act as a network former, strengthening grain boundaries by promoting inter-particle bonding, possibly through the introduction of a glassy phase or the formation of mullite at grain boundaries. However, the materials containing zircon batch 2 are being progressively sintered by the increasing amounts of fine silica present from the abrasion and erosion of the silica mill media and lining. This resulted in a more consolidated and, hence, stronger ceramic, see Section 3.4.

The materials containing zircon batch 3 initially showed a trend of increasing strength with increasing addition, indicating a similar mechanism to zircon batch 1, as a result of this zircon also being milled with alumina, although performed wet. The strength drop observed with additions beyond 15 wt% was then due to the presence of increasingly large amounts of zircon between the silica grains. The zircon prevented adjacent particles sintering together during the test and hence did not allow as much strengthening to occur, since zircon does not sinter as readily as silica at these temperatures.

3.3. Zircon batch effect on creep resistance at 1475 °C

The addition of zircon batches 1 and 2 had the effect of significantly reducing the creep of the ceramics at 1475 °C with a 3.2 N applied load. This was most likely due to an increase in inter-particle bonding caused by the alumina contamination or sintering caused by silica contamination from the mill process, see Fig. 5. The use of zircon batch 3 initially showed a very low value for creep, due to the larger effect of the finer alumina produced through wet milling. However, addition of more than 15 wt% appeared to increase the creep. This was due to decrease in silica particle bonding caused by the large amounts of zircon between the silica particles.

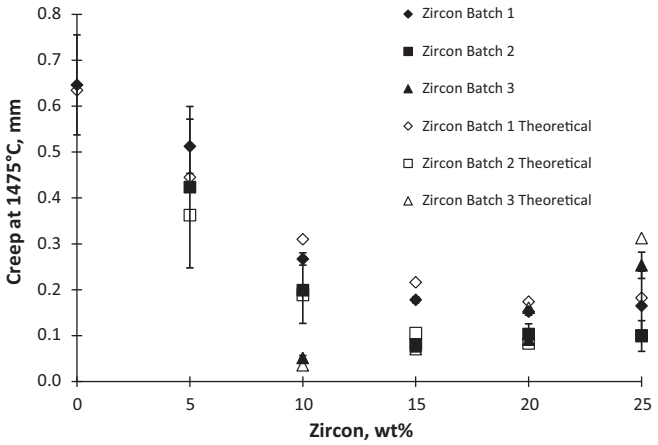

Fig. 5. Actual creep values and calculated creep values using Eq. (1) data for the materials containing the different zircon batches and in different amounts.

The silica powder used was also milled with alumina media and so, also, contained a certain level of alumina from the abrasion of the milling media. This, combined with the alumina [or ultra-fine abraded silica] from the milling of the zircon would be expected to have a predictable influence on the creep of these materials. However, since the majority of the alumina contamination associated with the zircon would be localised on the zircon particles surface it would have less of an effect than the well dispersed alumina on the surface of the silica powder.

Hence, a relationship is proposed that would depend on the alumina content of the zircon, the alumina concentration of the silica and the zircons surface area and concentration, in order to account for the effect of large amounts of fine zircon between the grains. The proposed relationship is given by Eq. (1). Where Al_{Si} is the total alumina from silica powders in %, Al_{Zr} is the total alumina from zircon powders in %, x is a zircon dependent factor that depends on milling process, source, mill media, etc. (Where $x = 1$ for zircon batch 1, 10 for zircon batch 2 and 25 for zircon batch 3), a is the surface area of the zircon in $m^2\,g^{-1}$ and $Zr_{wt\%}$ is the wt% addition of zircon.

$$\text{Creep} \quad (\text{mm}) = 1.1 \times 10^{-4}(Al_{Si} + x \cdot Al_{Zr}^{3/2})^{7/2} + \frac{a \cdot Zr_{wt\%}^{3}}{1 \times 10^{-5}} \tag{1}$$

3.4. Zircon batch effect on high temperature consolidation

All materials exposed to the dilatometry test contracted during the procedure, this was due to the sintering of the materials during the test. Table 2 shows the variation in total contraction for the different zircon batches and different amounts of zircon used. The material with no zircon addition contracted by precisely 0.5% during the test, the addition of just 5 wt% of zircon batches 1 and 2 increased this, with the addition of 5 wt% zircon batch 2 increasing this significantly to 2.13% compared to 0.90% for zircon batch 1. This was most likely due to the ultra-fine silica present from the mill procedure increasing the sintering rate. The total shrinkage then progressively decreased with increasing zircon addition.

The zircon appeared to be progressively preventing high temperature shrinkage in increasingly larger amounts. This was most likely a manifestation of the Zener effect, whereby a non-reactive secondary phase particle prevents grain boundary movement by introducing a drag force at the grain boundaries, F_d. This depends on both the amount of secondary phase and the surface energy of the secondary phase according to Eq. (2).[16] Where f_v is the volume fraction of the secondary phase, v_b is the surface energy of the secondary phase and r is the average particle radius of the secondary phase.

$$F_d = \frac{3 f_v v_b}{2r} \tag{2}$$

The materials containing zircon batch 3 can be seen to contract considerably less than those containing zircon batches 1 and 2. This was due to the significantly larger surface area of this zircon batch.

3.5. Effect of zircon on the crystallisation of fused silica

The cristobalite content of the ceramics, as measured by XRD, varied after firing depending on the amount of zircon and the zircon batch, see Table 3. From this data it can be seen that the material containing zircon batch 3 appeared to have larger amounts of cristobalite after firing with the materials containing 20 wt% and 25 wt% exhibiting twice the cristobalite content of the materials with the equivalent amount of zircon batch 1 or 2. This suggested that either the additional zircon surface area was acting as a nucleator or that the contaminants present were pro-

Table 2
Thermal contraction data at 1250 °C during thermal cycle to 1600 °C for all zircon containing materials and the associated standard deviations (average of 4 measurements).

Zircon, wt% addition	Zircon batch 1		Zircon batch 2		Zircon batch 3	
	Mean dL at 1250 °C (%)	Standard deviation	Mean dL at 1250 °C (%)	Standard deviation	Mean dL at 1250 °C (%)	Standard deviation
0	0.518	0.229	–	–	–	–
5	0.901	0.083	2.129	1.214	–	–
10	0.809	0.220	1.025	0.942	0.885	0.258
15	0.732	0.101	0.508	0.237	0.482	0.153
20	0.221	0.076	0.314	0.339	0.284	0.145
25	0.345	0.240	0.326	0.227	0.324	0.244

Table 3
Post fire cristobalite data for materials containing different zircons.

Zircon (wt%)	Cristobalite with zircon batch 1 (wt%)	Cristobalite with zircon batch 2 (wt%)	Cristobalite with zircon batch 3 (wt%)
0	3.5		
5	2.9	–	–
10	3.1	2.3	5.2
15	4.5	5.1	5.6
20	4.7	4.0	8.2
25	4.8	2.8	8.9

moting cristobalite formation more readily than with the other two batches, since the contaminants would also have a larger surface area.

If zircon were to directly affect the crystallisation of a large silica grain the growth front into the silica would be expected to be larger in the presence of a zircon–silica interface. Optical polarising microscopy performed on samples that were as supplied and heat treated to 1475 °C for 1 h. From this the growth front of cristobalite into a silica grain at a silica–zircon interface could be observed, but no detectable difference in the morphology of the growth front could be seen, see Fig. 6. This suggested that either the zircon was only a subtle nucleator and its effects were undetectable with this experiment or that the crystallisation was being influenced by the inherent contamination and not the actual zircon surface.

The evolution of cristobalite with time was also investigated for the materials with 0, 10 and 20 wt% zircon of all batches. These materials were isothermally heat treated to 1475 °C for 5, 15, 30 and 60 min and their cristobalite levels determined. From this the half-time and Avrami exponents were determined. The half-time is the time taken for 50% of the available silica to transform into cristobalite and the Avrami exponent is derived from the Avrami equation that describes the transformation of one phase to another at constant temperature,[17] and is given by Eq. (3); where X_c is the fractional crystallinity of the sample, t is the time in seconds, k is a scaling constant and n is the Avrami exponent.

$$\ln(1 - X_c) = kt^n \tag{3}$$

The Avrami exponent can be split into two parts, n_l and n_g, where n_g is the growth mechanism, n_l is the nucleation mechanism and $n = n_l + n_g$. For three-dimensional growth, n_l has values ranging from 0 to 1, indicating a constant nucleation rate and pre-existing nuclei respectively and n_g has typical value between 1.5 and 3 indicating diffusion controlled growth and a constant growth rate, respectively.[18]

It has been noted in the literature that the morphology of cristobalite growth in silica ceramics is plate like in nature and that the growth morphology can be changed with the addition of nucleators and mineralisers.[19,20,21]

The half-times and Avrami exponents for the materials containing the different zircon batches are shown in Table 4. From this it can be seen that increasing the amount of zircon decreases the half-time considerably. However, materials containing zircon batch 3 can be seen to be considerably reduced over that of the material with no zircon.

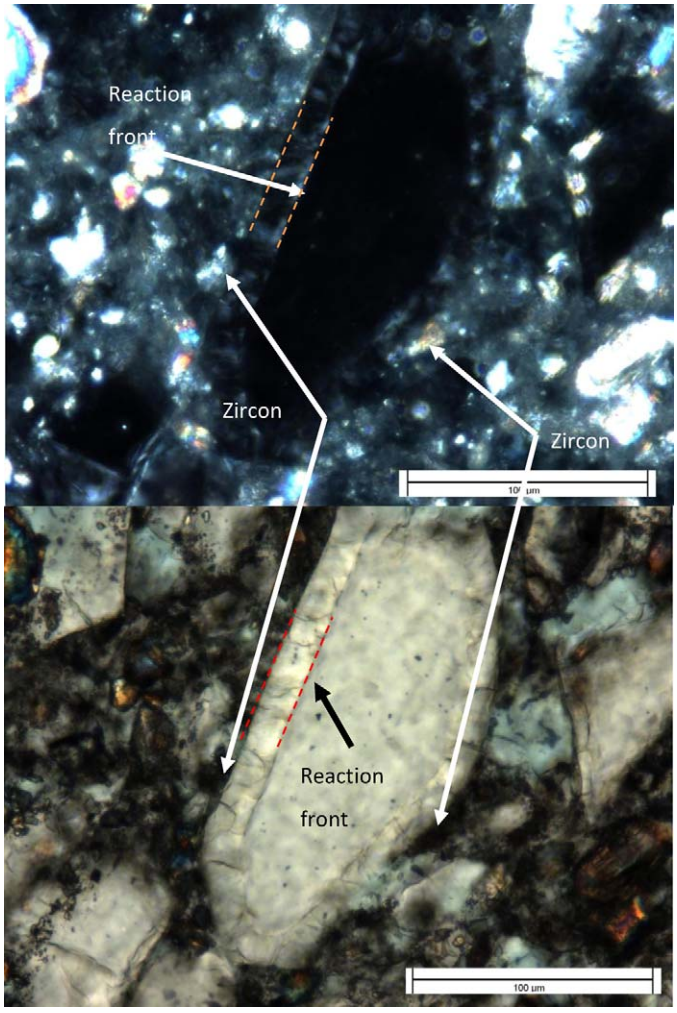

Fig. 6. Crystallisation of a large silica grain after 1 h at 1475 °C with adjacent large zircon particles (a) in plain polarised light and (b) in cross polarised light with a 1/4 wavelength advance, both 50× magnification.

Table 4
Avrami exponents and half-times for materials containing 0 wt%, 10 wt% and 20 wt% of zircon batches 1 and 3.

Zircon batch	Zircon (wt%)	Avrami exponent (n)	Half-time (s)
–	0	1.80	1552
1	10	1.93	1100
1	20	1.59	1070
2	10	1.91	1858
2	20	1.86	1216
3	10	1.31	686
3	20	1.22	517

The Avrami exponent appears to be similar for the material with no zircon and 10 wt% zircon batches 1 and 2. This is then reduced for materials with larger amounts of zircon and both the materials with zircon batch 3. The reduction in Avrami exponent suggested a change in growth mechanism.

An Avrami exponent of $n \approx 2$ suggested that the crystallisation was occurring at grain boundaries with sporadic disc

like growth, since the value is low it was most likely diffusion controlled and the nucleation mechanism was by pre-existing nucleation sites. The reduction in Avrami exponent from 1.80 with no zircon addition to 1.22 with 20 wt% of zircon batch 3 suggested a change in crystal growth morphology from disc shaped to rod shaped. The reduction in exponent suggested an increase in nucleation sites but it was unclear if this was due to the zircon or the alumina. However, examination of the Avrami exponent of the materials containing zircon batch 2 suggested that the crystallisation was due to alumina, since these materials showed little change with the different amounts of zircon, and had the lowest level of alumina contamination.

4. Conclusion and discussion

The contamination of zircon with a fine constituent from the milling procedure of raw material production has been linked to variation in the material properties of silica ceramics that utilise the zircon in their formulation. Increasing the amount of zircon increases the influence of these species and can have beneficial effects on material properties, such as flexural strength at 1475 °C and creep resistance at the same temperature.

The use of alumina grinding media results in an ultra-fine alumina constituent of the zircon that acts to increase inter-particle bonding, either by the introduction of a glassy phase or by the formation of mullite in very small quantities, which acts to increase the strength and creep resistance of the ceramics at elevated temperatures. However, detection of this phase has not been confirmed due to the low amounts present and the techniques employed, it is possible that TEM could be used to detect this phase at the grain boundaries. Silica grinding media acts result in an ultra-fine silica constituent of the zircon which, during hot testing, acts to increase the sintering rate due to its high surface energy and, consequently, causes an increase in strength/creep resistance.

Zircon was also shown to act as a Zener pinning agent at high temperature by acting as an inert secondary phase which introduces a pinning force at the grain boundaries and prevents consolidation. This was apparent from dilatometry measurements and also explained the strength and creep results of the fine, wet milled zircon batch, since this effect was larger for materials with higher surface areas.

The zircon was also determined to affect the crystallisation of fused silica. However, it is suggested that the zircon does not act as a nucleator, as put forward in previous literature but only enhances crystallisation through the inherent contamination present from the mill procedure used to grind the particles to the correct size distribution.

Acknowledgements

This research was made possible through funding from the EPSRC and Ross Ceramics Ltd., UK, and support from the University of Birmingham Centre for Formulation Engineering.

References

1. Jones S, Bentley SA, Marquis PM. Effect of refractory phase separation on investment mould integrity. *Br Ceram Trans* 2002;**101**:100–5.
2. Shi Y, Huang X, Yan D. Synthesis and characterisation of ultrafine zircon powder. *Ceram Int* 1998;**24**:393–400.
3. Hoskin PWO, Schaltegger U. The composition of zircon and igneous and metamorphic petrogenesis. *Rev Minerol Geochem* 2003;**53**:27–62.
4. Lee JH. Ternary phase analysis of interfacial silicates grown in HfO_x/Si and Hf/SiO_2/Si systems. *Thin Solid Films* 2005;**472**:317–22.
5. Caruba R, Baumer A, Ganteaume M, Iacconi P. An experimental study of hydroxyl groups and water in synthetic and natural zircons: a model of the metamict state. *Am Miner* 1985;**70**:1224–31.
6. Ewing RC. The metamict state: 1993—the centennial. *Nucl Instrum Meth B* 1994;**91**:22–9.
7. Meldrum A, Wang L, Weber WJ, Corrales LR, Ewing RC. Radiation effects in zircon. *Rev Minerol Geochem* 2003;**53**:387–425.
8. Awaad M, Kenawy SH. Sintering of zircon: the role of additives. *Br Ceram Trans* 2003;**102**:69–72.
9. Kuwahara Y, Suzuki K, Azuma N. Increase of impurity during fine grinding. *Adv Powder Technol* 1990;**1**:51–60.
10. Gammage RB, Glasson DR. Wear of mill components during the ball milling of calcium carbonate. *J Colloid Interface Sci* 1979;**71**:522–5.
11. Austin LG, Klimpel RR. Ball wear and ball size distributions in tumbling ball mills. *Powder Technol* 1985;**41**:279–86.
12. Tkacova K, Stevulova N, Lipka J, Sepelak V. Contamination of quartz by iron in energy-intensive grinding in air and liquids of various polarity. *Powder Technol* 1995;**83**:163–71.
13. Perez-Rodriguez JL, Perez-Maqueda LA, Justo A, Sanchez-Soto PJ. Influence of grinding contamination on high-temperature phases of pyrophyllite. *J Eur Ceram Soc* 1993;**11**:335–9.
14. Zevin LS, Kimmel G. *Quantitative X-ray diffractometry*. New York: Springer-Verlag Inc.; 1995.
15. Ek S, Root A, Peussa M, Niinisto L. Determination of the hydroxyl group content in silica by thermogravimetry and a comparison with H MAS NMR results. *Thermochim Acta* 2001:201–12.
16. Kang SJL. *Sintering, densification, grain growth & microstructure*. Elsevier Butterworth-Heinemann; 2005. p. 07506–63855.
17. Hurle DTJ. *Handbook of crystal growth 2. Part B: Growth mechanisms and dynamics*. North-Holland; 1994.
18. Bruna P, Crespo D, Gonzalez-Cinca R. On the validity of avrami. Formalism in primary crystallization. *J Appl Phys* 2006;**100**:054907.
19. Wang LY, Hon MH. The effect of cristobalite seed on the crystallization of fused silica based ceramic core. *Ceram Int* 1995;**21**:187–93.
20. Wang LY, Hon MH. The effects of zircon addition on the crystallisation of fused silica—a kinetic study. *J Ceram Soc Jpn* 1994;**102**:517–21.
21. Wereszczak AA, Breeder K, Ferber M, Kirkland TP, Payzant EA, Rawn CJ, et al. Dimensional changes and creep of silica core ceramics used in investment casting of superalloys. *J Mater Sci* 2002;**37**:4235–45.